



HAL
open science

Electro Fenton removal of clopyralid in soil washing effluents

María Belén Carboneras Contreras, Florence Fourcade, Aymen Assadi,
Abdeltif Amrane, Francisco Jesus Fernandez-Morales

► **To cite this version:**

María Belén Carboneras Contreras, Florence Fourcade, Aymen Assadi, Abdeltif Amrane, Francisco Jesus Fernandez-Morales. Electro Fenton removal of clopyralid in soil washing effluents. *Chemosphere*, 2019, 237, pp.124447. 10.1016/j.chemosphere.2019.124447 . hal-02280865

HAL Id: hal-02280865

<https://univ-rennes.hal.science/hal-02280865>

Submitted on 16 Dec 2019

HAL is a multi-disciplinary open access archive for the deposit and dissemination of scientific research documents, whether they are published or not. The documents may come from teaching and research institutions in France or abroad, or from public or private research centers.

L'archive ouverte pluridisciplinaire **HAL**, est destinée au dépôt et à la diffusion de documents scientifiques de niveau recherche, publiés ou non, émanant des établissements d'enseignement et de recherche français ou étrangers, des laboratoires publics ou privés.

1 **Electro Fenton removal of clopyralid in soil washing effluents**

2

3 María Belén Carboneras Contreras^{1,2}, Florence Fourcade^{2*}, Aymen Assadi², Abdeltif
4 Amrane², Francisco Jesus Fernandez-Morales^{1*}

5

6 (1) Chemical Engineering Department. Research Institute for Chemical and
7 Environmental Technology (ITQUIMA). University of Castilla- La Mancha, 13071,
8 Ciudad Real, Spain

9 (2) Univ Rennes, Ecole Nationale Supérieure de Chimie de Rennes, CNRS, UMR 6226,
10 F-35000 Rennes, France

11

12

13

14 *Corresponding authors:

15 **Francisco Jesus Fernández Morales**

16 University of Castilla-La Mancha, ITQUIMA, Chemical Engineering Dept., Avda.
17 Camilo José Cela S/N 13071, Ciudad Real, Spain
18 Tel: 0034 926 295300 (ext. 6350), Fax: 0034 926 295242
19 E-mail: fcojesus.fmorales@uclm.es
20 Orcid iD: 0000-0003-0389-6247

21

22 **Florence Fourcade**

23 University of Rennes, Ecole Nationale Supérieure de Chimie de Rennes, CNRS, UMR
24 6226, F-35000 Rennes, France
25 E-mail: florence.fourcade@univ-rennes1.fr

26

27 **Abstract**

28 The removal of a commercial herbicide, based on clopyralid, by means of Electro-Fenton
29 (EF) was studied using a soil washing effluent obtained using synthetic ground water as
30 washing fluid. From the results, it was observed that the degradation and mineralization
31 yields of clopyralid were high, even without the addition of supporting electrolyte. The
32 groundwater could be then used as a sustainable supporting electrolyte. The influence of
33 the minerals constituents, the current and the ferrous ions regeneration was evaluated.
34 The highest hydrogen peroxide production was achieved working at 200 mA but
35 regeneration of ferrous ions was not efficient at this current. Iodide ions were one of the
36 main responsible in the EF efficiency decrease due to their reaction with the produced
37 hydrogen peroxide. Electrochemical study proved that clopyralid was not electroactive
38 and that its degradation was mainly due to radical oxidation. Long duration electrolysis
39 carried out at 200 mA in groundwater provided an improvement of the solution
40 biodegradability after 480 min that can be linked to a significant increase in the carboxylic
41 acids production. These results support the feasibility of applying an EF process in order
42 to carry out a subsequent biological mineralization.

43

44 **Keywords:** Electro-Fenton; clopyralid; groundwater; soil washing effluent;
45 biodegradability improvement.

46

47 1. INTRODUCTION

48 The pollution related to the use and production of pesticides is an issue which not only
49 has impact on the environment but also concerns human beings and wildlife. The
50 application of pesticides is an essential tool for the correct development of crops, however
51 it became a serious problem during the green revolution, increasing the loss of soil
52 fertility, the soil acidification, the nitrate leaching, the resistance of weed species and the
53 loss of biodiversity (Tilman et al., 2002; Verma et al., 2013; Verma et al., 2014).
54 Additionally, according to the literature (Pimentel and Levitan, 1986), less than 0.1% of
55 pesticides applied for pest control reach their target pests. It means that more than 99.9%
56 of pesticides move into the environment, polluting water, soil and air. Water pollution by
57 pesticides is a widespread problem. Several pesticides haven been detected in surface and
58 groundwater, as it has been described by a great number of research studies (Bortleson
59 and Davis, 1997; Aydin et al., 2018; Xie et al., 2019). Moreover, human health is
60 significantly affected by this kind of pollution, producing, among other problems, fertility
61 diseases (Cano-Sancho et al., 2019).

62 The removal of organic pollutants from waters has been studied during years and it is a
63 topic which can be faced by using different technologies, from the adsorption of the
64 pollutants on carbon materials (Liu et al., 2018) to the use of microorganisms to degrade
65 the organic compounds (De Lucas et al., 2007; Garcia-Becerra and Ortiz, 2018; Gaur et
66 al., 2018; Kumar et al., 2018). One of the most effective technologies to remove organic
67 molecules from water is the Advanced Oxidation Process (AOP). They are defined as
68 processes which involve the generation of highly reactive oxidizing species able to attack
69 and degrade organic substances. This concept was established in the 1980s (Glaze, 1987;
70 Huang et al., 1993). The AOP processes have demonstrated good efficiencies treating

71 relatively low volumes of effluents at high concentrations. For this reason, they can be
72 used after a concentration step such as membrane separation or adsorption processes
73 (Pérez et al., 2010; Urtiaga et al., 2013; Wang et al., 2014; Liang et al., 2016; Bouaziz et
74 al., 2017; Aboudalle et al., 2018a). One class of AOPs that is gaining attention over the
75 last two decades are the electrochemical advanced oxidation processes (EAOPs)
76 (Comninellis et al., 2008; Barrera-Díaz et al., 2014; Chaplin, 2014; Moreira et al., 2017).
77 The main advantages of the EAOPs versus traditional AOPs are that this kind of
78 technology is able to manage a wide range of pollutants and concentrations, can in situ
79 generate H₂O₂, operates at mild conditions and can be easily scalable, amongst others.
80 Additionally, this technology provides some upsides for the prevention and remediation
81 of pollution problems because the electron is a non-polluting reagent (Sirés et al., 2014).
82 Nevertheless, EAOPs have associated important downsides such as the electrical costs
83 related to the energy supply and the consumption of chemicals as supporting electrolyte
84 (Oller et al., 2011; Sirés et al., 2014). In order to reduce the costs of the EAOP processes,
85 they can be coupled with cheap treatments such as the bioprocesses. The order in which
86 the EAOP and the bioprocess are combined attends to different factors such as the
87 biodegradability/toxicity of the effluents, the nature of the pollutant and the existence of
88 acclimatized microbial cultures able to degrade the target pollutant amongst others (Oller
89 et al., 2011; Ganzenko et al., 2014).

90

91 Electro-Fenton (EF) process is considered one of the most efficient EAOPs processes.
92 The EF process is based on the electrogeneration of H₂O₂ at the cathode by reducing the
93 fed dissolved oxygen. The addition of an iron catalyst and an acid pH are necessary
94 conditions to produce oxidant •OH in the liquid bulk (Brillas et al., 2009; Barrera-Díaz et
95 al., 2014; Aboudalle et al., 2018a). Fenton`s reaction involves H₂O₂ and ferrous iron to
96 form •OH Eq. (1).



98 Electrochemical processes are usually characterized by the requirement of a supporting
99 electrolyte, mineral salts which provide to the solution enough conductivity in order to
100 decrease the cell voltage. However, the addition of mineral salts attained one important
101 drawback, because in spite of improving the conductivity, it increases the pollution of the
102 water (Belen Carboneras et al., 2018). Because of that, novel solutions must be reached.

103 In this context, this study focuses on the examination of the main parameters influencing
104 the clopyralid removal and mineralization by means of the EF process. Moreover, a study
105 of the influence of the operational variables over the enhancement of the biodegradability
106 of the effluent caused by the EF process was carried out.

107 The EF clopyralid oxidation was implemented with and without the addition of any
108 supporting electrolyte. To do that, a synthetic groundwater solution was used as soil
109 washing fluid to enhance the conductivity, taking the advantage of this sustainable and
110 non-polluting natural resource.

111

112 **2. MATERIALS AND METHODS**

113 **2.1. Chemicals and soil washing effluents**

114 In this work, the selected target pollutant was clopyralid. It was used in its commercial
115 formulation, Lontrel[®] 72 (72% w/w), and was supplied by Dow AgroSciences. The
116 polluted effluents used in this research were synthetic soil washing effluents. The soil
117 washing fluid used to extract the pollutant from the soil was groundwater. According to
118 the composition and concentration of typical groundwater and the results described in the
119 literature (Minerales, 1985; Chair et al., 2017a; 2017b), the synthetic effluent presented
120 the following concentrations: Na₂SO₄ 50 mM; MgSO₄ 7H₂O 5.54 mM; NaCl 2.25 mM;
121 NaNO₃ 1.53 mM; KI 0.15 mM; CaCO₃ 12.47 mM.
122 FeSO₄·7H₂O (purity 99%), Na₂SO₄ and the rest of the chemicals used in this work were
123 purchased from Acros Organics (Thermo Fisher Scientific, Geel, Belgium).
124 In the literature, it has been described that the optimum pH to carry out the EF process is
125 3 (Diagne et al., 2007). Because of that, the pH of the wastewater was adjusted to 3 before
126 the experiments by adding analytical grade sulfuric acid H₂SO₄ purchased from Acros
127 Organics. All the solutions were prepared using Ultrapure water (Millipore Elga).

128

129 **2.2. Electrochemical Apparatus and Procedures**

130 The electrochemical reactor consisted of a batch undivided cylindrical glass compartment
131 with a volume of 800 mL. The main components of the electrochemical cell were a
132 cylindrical platinum anode (32 cm²), which was placed at the centre of the reactor and a
133 tri-dimensional piece of carbon felt of 112 cm² of geometrical area (Le Carbone Loraine
134 RVG 4000 Mersen, Paris la Défense, France), which acted as cathode. The carbon felt
135 electrode surrounded the platinum anode so as to get a good potential distribution. The
136 main carbon felt characteristics were 35.3 m² g⁻¹ of specific area, 500 g m⁻² of area weight,
137 thickness of 0.4 cm and 95% of porosity). Before starting the electrolysis, compressed air
138 was bubbled into the solution during 15 min in order to provide the solution with an

139 appropriated O₂ concentration. The experiments were carried out in duplicate, at 20 °C
140 and galvanostatic conditions. The current was applied using a DC power supply (Metrix,
141 model AX 322-Chauvin Arnoux Group, Paris, France). Just before the beginning of the
142 EF reactions the catalytic Fe²⁺ was added into the reaction bulk as FeSO₄·7H₂O. The Fe²⁺
143 concentrations studied were 0.1, 0.5, 1, 2 and 5 mM.

144 In order to select the optimal operating conditions in terms of clopyralid degradation and
145 mineralization, several experiments were made changing one of the main parameters
146 influencing the EF process, the current applied. In the literature it has been described that
147 the current governs the formation of H₂O₂, the regeneration of ferrous iron and therefore
148 the production of hydroxyl radicals (Oturán et al., 2008; Özcan et al., 2009; Feng et al.,
149 2014; Aboudalle et al., 2018b).

150

151 **2.3. Analytical procedure**

152 *2.3.1. High performance liquid chromatography (HPLC)*

153 Clopyralid concentration was measured by HPLC using a Waters 996 system equipped
154 with a Waters 996 PDA (Photodiode Array Detector) and Waters 600LCD Pump. The
155 column was a Waters C-18 (4.6 mm x 250 mm x 5 µm). Acetonitrile (purity 99.9%)
156 (HPLC grade) was purchased from Sigma Aldrich (Saint Quentin Fallavier, France). The
157 mobile phase was a mixture of acetonitrile/ultra-pure water (20/80 v/v) with 0.1% of
158 formic acid. The flow rate was 1 mL min⁻¹ and the herbicide was detected at 280nm.

159

160 *2.3.2. Total organic carbon (TOC)*

161 TOC concentration was monitored by means of a TOC-V_{CPH/CPG} Total Analyser
162 Shimadzu. Organic Carbon compounds were combusted and converted to carbon
163 dioxide; then it was detected by a Non-Dispersive Infra-Red (NDIR) Detector.

164

165 *2.3.3. Ion chromatography (IC)*

166 The carboxylic acids generated during the electrolysis were identified and quantified by
167 a DIONEX DX120 ion chromatography. The chromatograph was equipped with a
168 conductivity detector, using an anion exchange column AS19 (4 mm x 250 mm) as the
169 stationary phase, and solutions of KOH in water, prepared from KOH (12 M), as the
170 mobile phase. The analysis were carried out using a gradient elution mode, starting with
171 10 mM KOH during 10 min and then increasing linearly to 45 mM from 10 to 25 min.
172 Finally, from 25 to 35 min the concentration of KOH was 45 mM. The flow rate was set
173 at 1 mL min⁻¹.

174

175 *2.3.4. Ferrous ions and H₂O₂ concentrations*

176 The ferrous ions concentration in the reactor was measured by means of a colorimetric
177 principle, according to the Phenanthroline Method NF 90-017 (AFNOR, 1982). The
178 concentration of H₂O₂ was determined by the potassium titanium (IV) oxalate method
179 according to standard DIN 38 409, part 15, DEV-18 (Eisenberg, 1943).

180

181 *2.3.5. Chemical oxygen demand (COD) measurements*

182 CSB Nanocolor[®] tests were employed to analyse the COD of the samples. They were
183 supplied by Macherery-Nagel (Düren, Germany).

184

185 *2.3.6. Biochemical oxygen demand (BOD₅) measurements*

186 In order to evaluate the influence of the EF process on the biodegradability of the soil
187 washing effluents, BOD₅ test were carried out using Oxitop ISA technology (from WTW,
188 Alés, France). The tests were performed under the normalised conditions; 5 d at 20 °C.

189 Before the test, it was necessary to adjust the pH of all the samples at 7 by adding NaOH.
190 The inoculum required to perform the analyses was collected from the municipal
191 wastewater treatment plant (Rennes Beaurade, France). For inoculation of the bottles, an
192 initial biomass concentration of 0.05 g L^{-1} was necessary. The following trace mineral
193 were used to ensure the nutrients availability along the BOD₅ tests (g L^{-1}): $\text{MgSO}_4 \cdot 7\text{H}_2\text{O}$,
194 22.5; CaCl_2 , 27.5; FeCl_3 , 0.15; NH_4Cl , 2.0; Na_2HPO_4 , 6.80; KH_2PO_4 , 2.80.
195 To check the viability of the seed used as inoculum, a control test containing glutamic
196 acid (150 mg L^{-1}) and glucose (150 mg L^{-1}) was carried out. Additionally, a blank test, in
197 absence of carbon source, was performed in order to determine the endogenous oxygen
198 consumption.

199

200 *2.3.7. Electrochemical analysis*

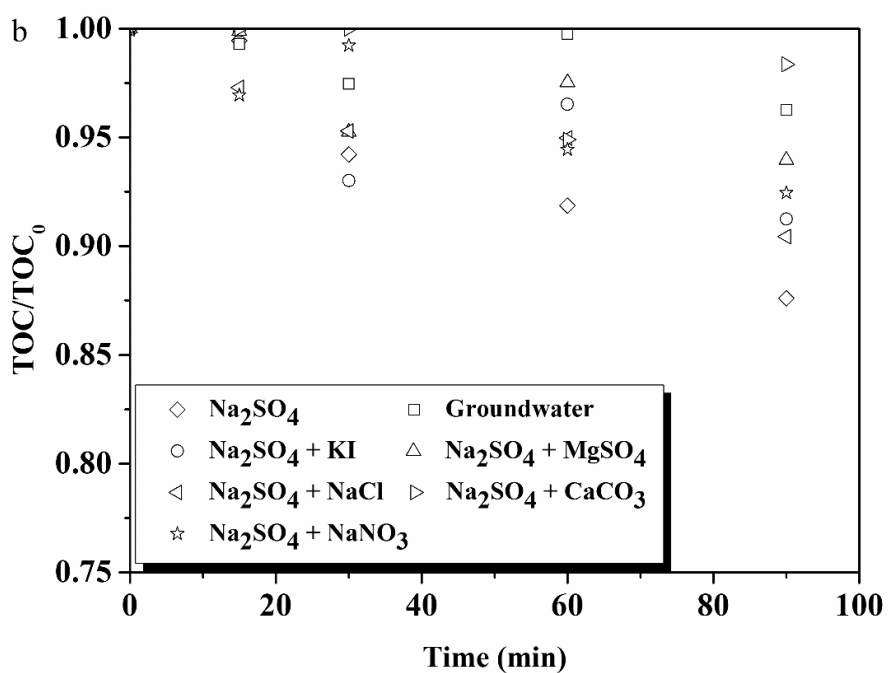
201 Voltammograms were obtained in a conventional three-electrodes cell with a scan rate of
202 100 mV s^{-1} using a BioLogic SP-150 potentiostat recorded to EC-Lab V10.36 software.
203 As working electrode both, platinum and vitreous carbon, were tested. The platinum
204 electrode (3.14 mm^2) was used to characterize the anodic oxidation processes while the
205 carbonous electrode (7.07 mm^2) was used to study the cathodic reduction processes. In
206 both cases, a Pt wire was used as the counter electrode and all the electrode potentials
207 were measured with respect to a saturated calomel electrode (SCE) located near to the
208 working electrode. Experiments were performed at ambient temperature under nitrogen
209 atmosphere to avoid dissolved oxygen.

210

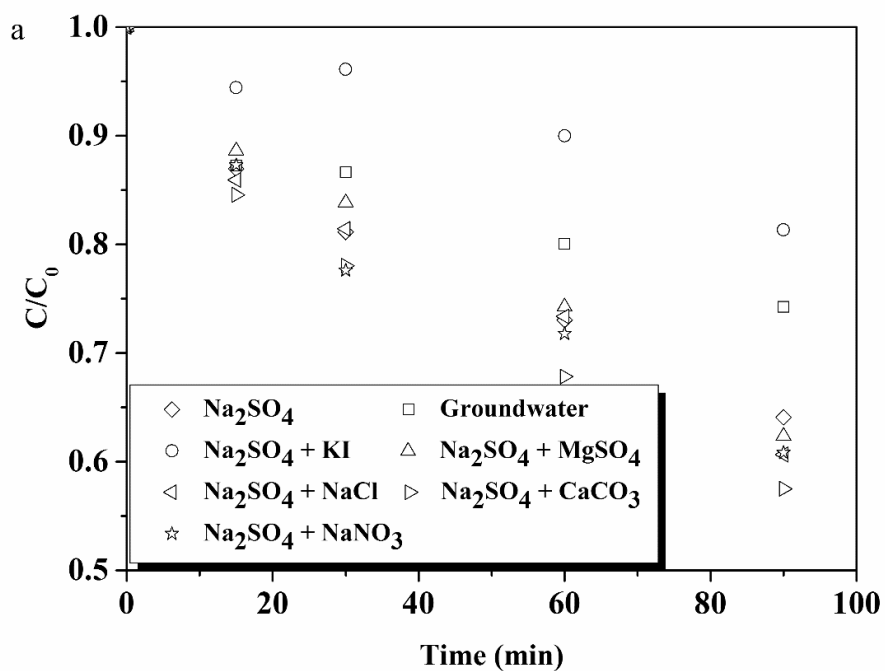
211 **3. RESULTS AND DISCUSSION**

212 **3.1. Effect of the mineral salts contained in the groundwater on the EF experiments**

213 Considering the composition of the soil washing solution, it must be highlighted that from
214 a thermodynamic point of view, redox reaction between the constituents cannot occur.
215 From Fig. 1, it can be seen that the composition of the supporting electrolyte directly
216 affected the clopyralid degradation and mineralization. As previously stated, the use of
217 groundwater could be a sustainable option for soil washing processes. In order to check
218 the influence of the different mineral salts, a set of experiments were carried out. To do
219 these experiments, 7 different electrolyte solutions were used. The first electrolyte
220 solution contained all of the components of the synthetic groundwater (Chair et al.,
221 2017b). As a reference, a tests containing the typical electrolyte solution, 50 mM Na₂SO₄,
222 was carried out. Finally, with the aim to study the individual contribution of the minerals
223 contained in the synthetic ground water, 5 extra electrolyte solutions were prepared.
224 These electrolytes were based on the typical supporting electrolyte, 50 mM Na₂SO₄, but
225 including in each case one of the minerals contained in the groundwater. The reaction
226 conditions were 0.1 mM of Fe²⁺, 50 and 100 mA of current. These operational conditions
227 were identified as the optimum ones in a previous work carried out when operating with
228 a similar set-up (Dalle et al., 2017). The current intensities studied yield very similar
229 results. Because of that, only the results obtained at 50 mA are presented in Fig. 1.
230



231



232

233 Figure 1. Influence of the electrolyte composition on the degradation (a) and
 234 mineralization (b) of clopyralid (initial concentration 180 mg L⁻¹), 0.1 mM of Fe²⁺, 50
 235 mA of current and 0.1 mL min⁻¹ of compressed air.

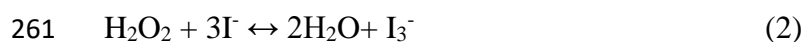
236 As can be seen in Fig. 1, the removal of the pollutant depended on the composition of the
237 electrolyte used. The influence was mainly visible for the clopyralid degradation, which
238 ranged from 20% to 40%. However, the mineralization yields presents very similar values
239 in all the cases, about 10%.

240 When the synthetic groundwater was used as electrolyte, average removal efficiencies
241 were obtained, presenting a removal rate of about $0.54 \text{ mg L}^{-1} \text{ min}^{-1}$.

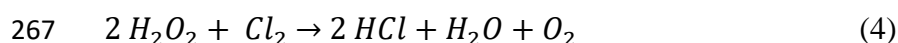
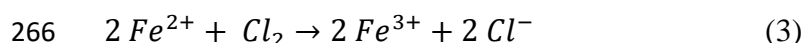
242 In most of the cases, except in the presence of iodide ions, the presence of single trace
243 mineral from the groundwater had a slightly influence on the average degradation rates,
244 presenting the best average removal rate the combination of the Na_2SO_4 and CaCO_3 , 0.93
245 $\text{mg L}^{-1} \text{ min}^{-1}$. This result indicates that these mineral ions, except the iodide ions, did not
246 interfere on the clopyralid degradation. In Fig. 1a, iodide ions clearly worsened the
247 clopyralid removal process. When the KI was present in the electrolyte, (groundwater
248 electrolyte and $\text{Na}_2\text{SO}_4 + \text{KI}$ electrolyte), only about 20% of the initial clopyralid was
249 degraded after 90 min.

250 With regard to the mineralization, the best mineralization yield was obtained when using
251 Na_2SO_4 as the sole supporting electrolyte. Anyway, the low mineralization observed in
252 all the cases during the electrolysis could be explained by the reaction between the
253 hydroxyl radicals and the inorganic compounds contained in the effluent. This reaction
254 involves simple electron transfer of $\bullet\text{OH}$ to form the hydroxide ion with the corresponding
255 change in the oxidation state of the donor (Buxton et al., 1988). Inorganic ions are
256 hydroxyl radical consumers, this statement justify the worse efficiency when mineral salts
257 were used.

258 In this sense it must be highlighted that, considering the standard potentials of H_2O_2 / H_2O
259 and I_3^- / I^- redox couple, iodide ions can react with the hydrogen peroxide produced at the
260 cathode surface Eq. (2) interfering with the Fenton reaction.



262 Another ion interfering the Fenton reaction was chloride ion. According the literature,
263 (Loaiza-Ambuludi et al., 2013) electrogenerated active chlorine can oxidize Fe^{2+} Eq. (3)
264 or decompose hydrogen peroxide Eq. (4), reducing the production rate of the strong
265 oxidant $\bullet OH$ by the Fenton's reaction (Beqqal et al., 2017).



268 It should be noted that to allow chloride ions oxidation, the potential of the anode needs
269 to be higher than about 1 V/SCE ($E^0 (Cl_2/Cl^-) = 1.24$ V/SHE) and then the production of
270 chlorine depends on the operating conditions and mainly on the applied current.

271

272 **3.2. Effect of the applied cathodic current on H_2O_2 production and ferrous** 273 **regeneration**

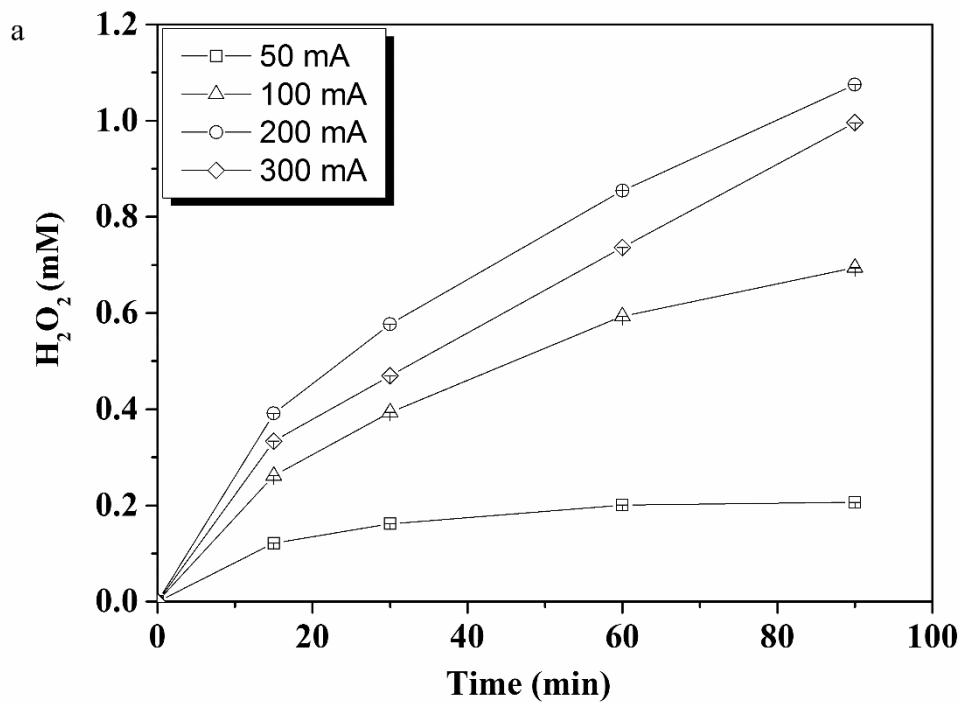
274

275

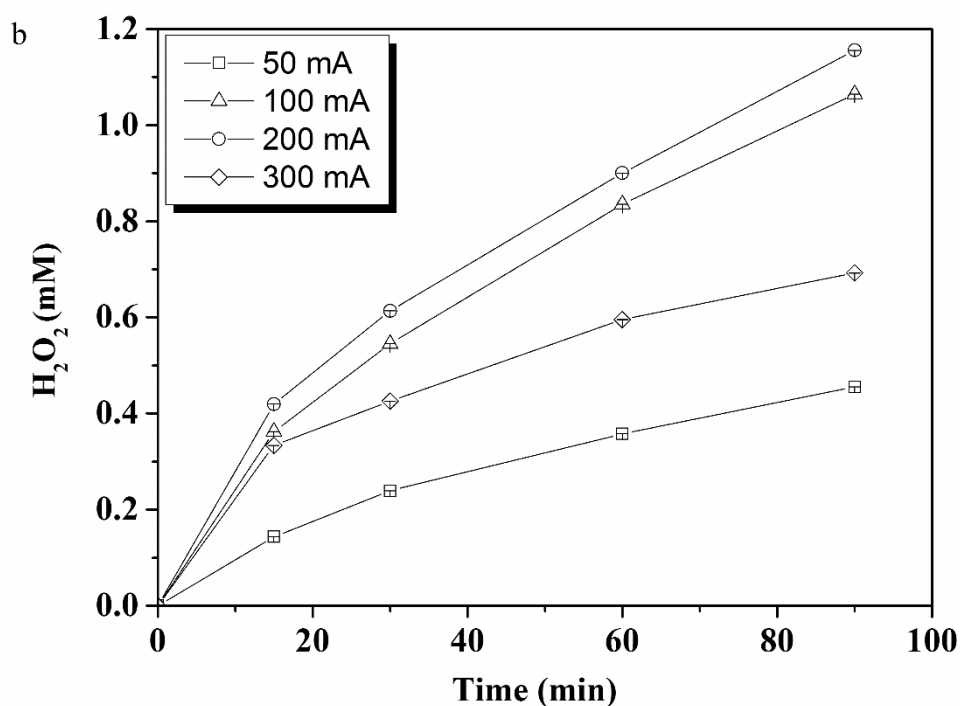
276 *3.2.1. Effect of the current on the H_2O_2 production*

277 Experiments were developed at different currents ranging from 50 to 300 mA. In these
278 experiments, synthetic groundwater was used as supporting electrolyte, during 90 min at
279 pH 3 and without the addition of Fe(II) and clopyralid to avoid EF reactions. The current

280 for H_2O_2 accumulation depended on some factors like reactor configuration, cathode
281 material and operation conditions. 3D carbonaceous cathodes, such as carbon felt, have
282 demonstrated good properties for H_2O_2 formation. Carbon is non-toxic, presents good
283 stability and low catalytic activity of H_2O_2 decomposition (Petrucci et al., 2016; Das and
284 Golder, 2017). The obtained results were compared with the same experiments using the
285 typical electrolyte in electrochemistry, Na_2SO_4 (50 mM), with the aim to evaluate the
286 influence of the mineral salts used as supporting electrolyte. The production of H_2O_2 as
287 function of the electrolysis length and applied current is presented in Fig. 2.



288

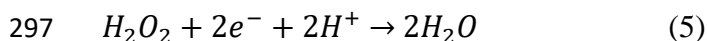
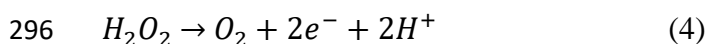


289

290 Figure 2. Effect of the current on the H₂O₂ production using (a) groundwater and (b) 50
 291 mM Na₂SO₄.

292

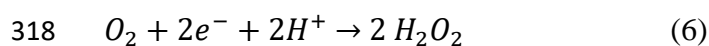
293 The H₂O₂ production was not linear along the experiment due to the occurrence of
 294 parasitic reactions, mainly anodic oxidation of H₂O₂ Eq. (4) and cathodic reduction to
 295 water Eq. (5) (Pérez et al., 2017; Zhou et al., 2018).



298 The evolution of the production of H₂O₂ during the experiment is directly related with the
 299 dissolved oxygen concentration. Usually, dissolved oxygen concentration remains
 300 constant at the beginning of the experiment until the polarization of electrodes takes place.
 301 After this stage, the concentration of dissolved oxygen in the solution depended on the
 302 applied current (Dalle et al., 2017).

303 The best H₂O₂ productions were achieved when working at 200 mA with both supporting
304 electrolytes: groundwater and Na₂SO₄. However, the concentrations reached with Na₂SO₄
305 as supporting electrolyte were higher compared with groundwater. The maximum
306 concentration of H₂O₂ obtained when working at 200 mA with Na₂SO₄ as supporting
307 electrolyte was about 1.16 mM; while it was about a 10% lower using groundwater at the
308 same current, reaching 1.08 mM. The difference could be, in part, explained by the
309 reaction of H₂O₂ with iodide ions contained in the groundwater can in part explain the
310 lower accumulated concentration.

311 Working with groundwater as supporting electrolyte, at 50 mA, the production of H₂O₂
312 increased during the first 30 min and then remained constant, showing the implementation
313 of an equilibrium between the anodic oxidation of H₂O₂ Eq. (5) and its cathodic
314 production Eq. (6). This effect was not observed at the other current applied, which
315 indicates that the production process outcompete the anodic oxidation process. Moreover,
316 the amount of O₂ produced at the anode, see Eq. (4), increases with the applied current
317 and then favours the production of hydrogen peroxide (Dalle et al., 2017).



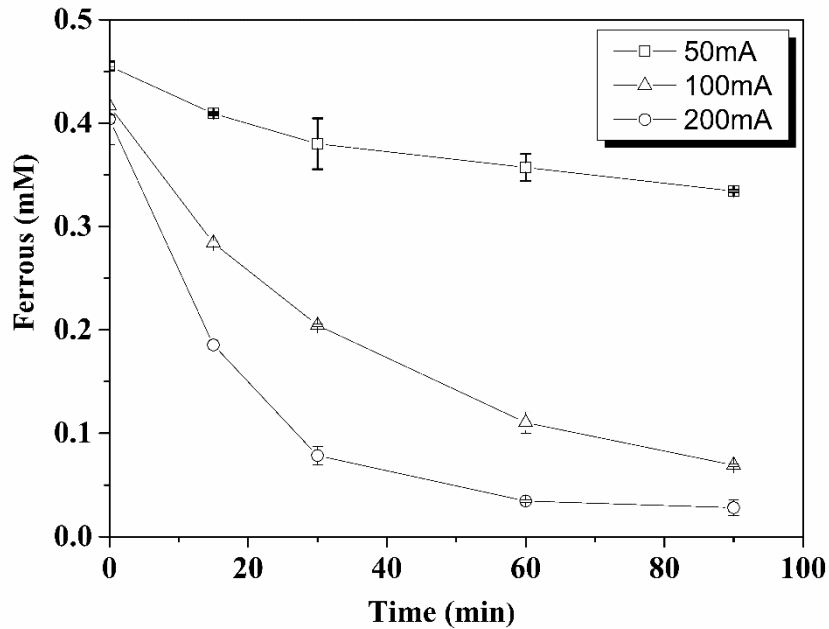
319 When operating at higher current densities, the H₂O₂ production increased. However, at
320 the highest applied current, 300 mA, the accumulation of H₂O₂ did not show a
321 proportional improvement. This behaviour could be explained because the reduction of
322 O₂ to form H₂O becomes preferential (Özcan et al., 2008).

323

324 **3.3. Effect of the current on ferrous ions regeneration**

325 The next step was the study of the ferrous ion regeneration when working with the
326 groundwater medium during 90 min at pH 3 without the addition of clopyralid. A series

327 of experiments at different current intensities were carried out with at an initial
328 concentration of Fe^{2+} of 0.5 mM. Fig. (3) shows the evolution of ferrous iron.



329

330 Figure 3. Effect of the applied current on the ferrous iron concentration.

331

332 In spite of getting the best H_2O_2 production at 200 mA, the worst regeneration of ferrous
333 ions is achieved at the same current. A decrease of ferrous ions concentration about 25%
334 was observed when the current reached 50 mA. For 100 and 200 mA a significant
335 decrease in total iron concentration took place after 90 min of electrolysis. The ferrous
336 iron concentration decreased from 0.45 to 0.07 and to 0.03 mM at 100 and 200 mA
337 respectively.

338 Some of the reasons which explain the bad performance of the highest current intensities
339 in the iron regeneration could be the followings:

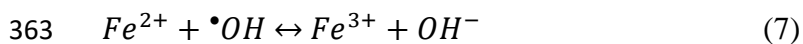
- 340 - Water reduction can lead to a local alkalization of the solution caused by hydroxyl
341 anions formation during H₂ release and then to the precipitation of iron as Fe(OH)₃
342 (Brillas et al., 2009; Petrucci et al., 2016).
- 343 - Iron hydroxide could be adsorbed onto the electrode surface or iron ions could be
344 reduced to metallic iron considering standard potentials for iron redox couples
345 (Aboudalle et al., 2018b).

346 These phenomena could explain a lower efficiency for the highest current densities.

347

348 **3.4. Effect of the initial Fe²⁺ on the EF experiments**

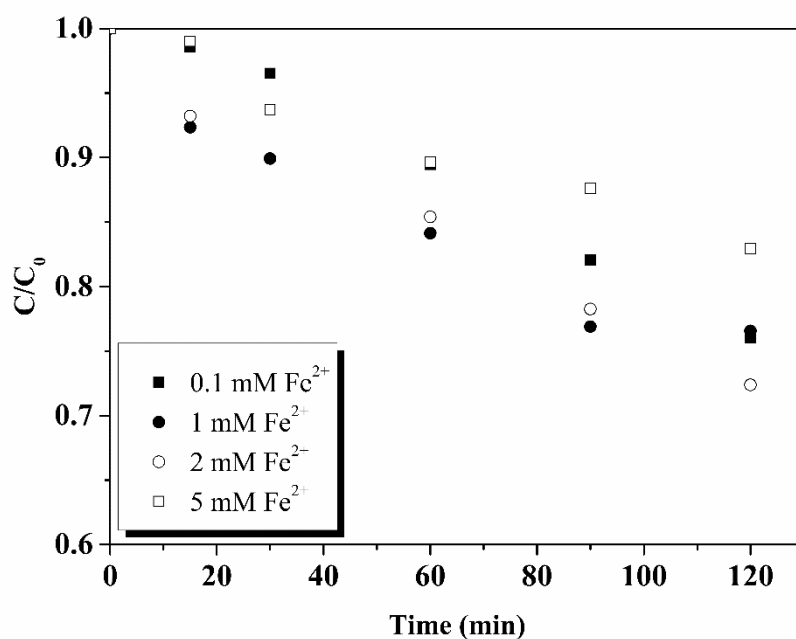
349 The initial ferrous ions catalyst concentration is another important parameter in the EF
350 process. Taking into account that the highest production of H₂O₂ was obtained at 200 mA,
351 even if the regeneration of the ferrous catalyst was not efficient throughout the
352 electrolysis, the influence of the initial concentration of FeSO₄·H₂O on the clopyralid
353 degradation was studied with 4 different initial concentrations of Fe²⁺ ranging from 0.1
354 to 5 mM. As reported in Fig. (4), the initial concentration of ferrous ions influenced the
355 degradation of the clopyralid, fluctuating the removal yield between 18 and 28%. Initial
356 concentrations of 0.1 and 1 mM caused about 25% of clopyralid degradation. The
357 clopyralid removal slightly increased when the initial concentration of Fe²⁺ was 2 mM
358 reaching a clopyralid removal percentage of about 28%. Finally, when the concentration
359 of Fe²⁺ was 5 mM the removal yield decreased to about 18%. This reduction in the
360 clopyralid removal could be explained by the competitive effects between hydroxyl
361 radicals, resulting from the Fenton`s reaction, and the excess of ferrous ions (Panizza and
362 Cerisola, 2009; Aboudalle et al., 2018b), according to Eq. (7).



364

365 If ferrous ions concentration had a little influence on the clopyralid degradation, the
366 mineralization of organic compound was not influenced by the catalyst concentration
367 (data not shown). It can be then concluded that the influence of the ferrous ion
368 concentration, within the range studied in this work, does not present a significant effect
369 on the clopyralid removal.

370 This statement is in accordance with other studies, where the initial catalyst concentration
371 does not have a strong influence in the degradation and mineralization of organic
372 pollutants (Loaiza-Ambuludi et al., 2013; Aboudalle et al., 2018b).



373

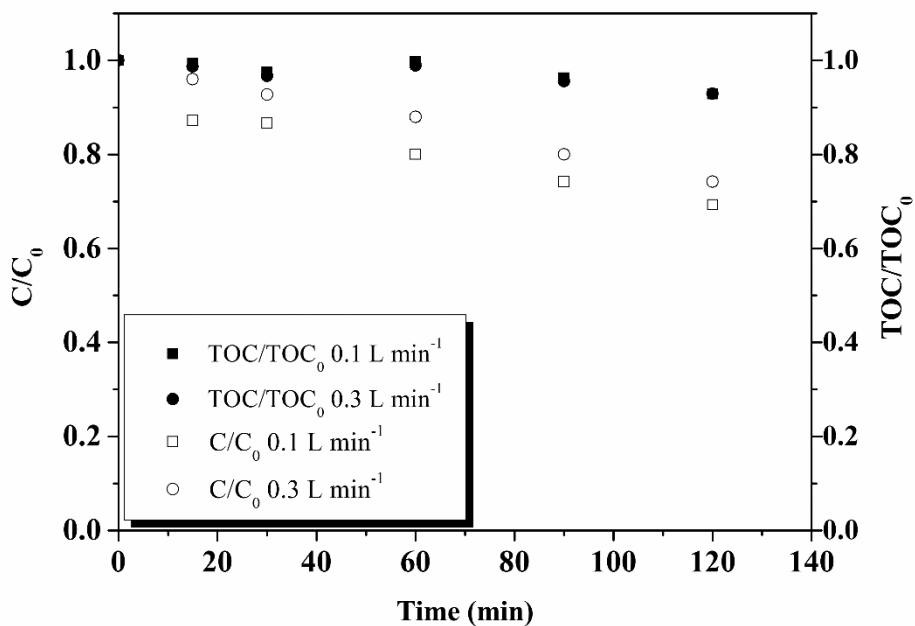
374 Figure 4. Influence of the initial Fe²⁺ concentration on the clopyralid degradation. Initial
375 clopyralid concentration 180 mg L⁻¹.

376

377

378 3.5. Effect of oxygen mass flow rate

379 One of the main reactions which manage EF is the cathodic reduction of oxygen to
380 generate H_2O_2 . Oxygen is transferred from the gaseous phase to the aqueous phase, and
381 the dissolved oxygen in the liquid bulk is transferred to the cathode surface, where the
382 reduction takes place. Consequently, it was expected that an increment in the oxygen flow
383 could enhance the mass transfer rate and therefore the subsequent reactions (Do and Yeh,
384 1996). In order to increase the availability of oxygen in the liquid bulk, the O_2 flow rate
385 was increased from 0.1 to 0.3 L min^{-1} . During the experiments, the current and the ferrous
386 concentration were kept at 50 mA and 0.1 mM , respectively. As can be seen in Fig. 5,
387 results indicate that an increment in the flow rate from 0.1 to 0.3 L min^{-1} had a slight
388 influence on the removal but not on the mineralization efficiency.



389

390 Figure 5. Effect of the oxygen mass flow on the removal efficiency. Clopyralid
391 concentration (full symbols) and TOC concentration (empty symbols).

392

393 As can be seen in Fig. 5, the mineralization achieved was almost identical in both cases,
394 whereas the clopyralid removal values were slightly different. Similar results were
395 obtained in research previously reported in the literature (Dalle et al., 2017), where it was
396 demonstrated that an increment from 0.5 to 3 L min⁻¹ has not an important influence on
397 the hydrogen peroxide production and hydroxyl radical concentration (Dalle et al., 2017).
398 This behaviour could be explained by the very similar saturation of oxygen in the liquid
399 bulk obtained in both cases (Dalle et al., 2017). In this sense, the slight enhancement
400 obtained when operating at 0.3 L min⁻¹ of oxygen flow rate could be explained by the
401 higher turbulence caused which leads to a higher mass transfer coefficient on the surface
402 of the electrode.

403

404 **3.6. Anodic reaction during clopyralid degradation**

405 In order to study the contribution of a direct oxidation and/or reduction of the clopyralid
406 at the electrode surfaces during the EF process, the electrochemical behaviour of the
407 target pollutant was also investigated. For this purpose, current potential curves were
408 plotted and electrolysis with and without tert-butanol were implemented. Tert-butanol is
409 used here as scavenger which reacts with hydroxyl radicals, generating inert
410 intermediates. These inert compounds cause the termination of the radical chain reaction
411 (Ma and Graham, 2000). The current potential curves, obtained by cyclic voltammetry,
412 were carried out with a vitreous carbon electrode ($S = 7.07 \text{ mm}^2$) as a working electrode
413 when the curves were plotted in reduction, a platinum electrode in oxidation ($S = 3.14$

414 mm²), a Pt counter electrode and SCE as reference electrode ($r = 100 \text{ mV s}^{-1}$). These
415 measurements were carried out under nitrogen atmosphere, at room temperature, pH 3
416 and at a clopyralid concentration of 180 mg L^{-1} . In order to isolate the behaviour of the
417 clopyralid two current potential curves were carried out, one of them with groundwater
418 as supporting electrolyte, and the other one with groundwater and clopyralid. The
419 obtained results are presented in Fig. SM-1 and did not show any clopyralid reaction at
420 the electrodes surface.

421 The current-potential curves did not show any signal in reduction with vitreous carbon
422 electrode (data not shown). With a platinum working electrode, a reversible signal
423 appeared in both curves, due to the oxidation of one of the ions in the groundwater. The
424 peak detected on the platinum anode took places at $+0.54\text{V}$ and could be related with the
425 oxidation of I^- into I_3^- . A signal was also observed around $+1 \text{ V}$ and can be attributed to
426 the oxidation of chloride ions. In this case, the formation of chlorine during the
427 electrolysis can influence the production of hydroxyl radicals.

428

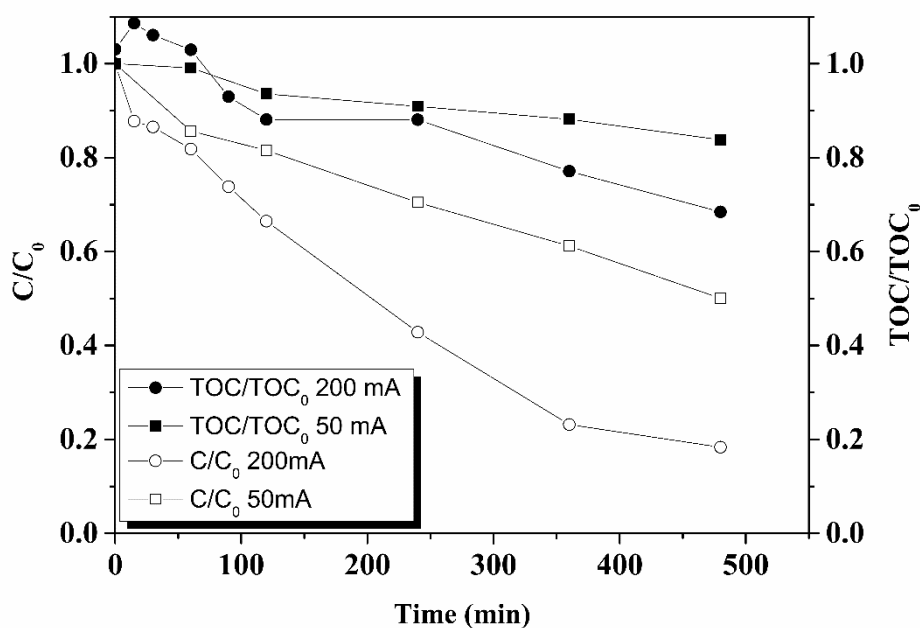
429 Besides this analysis, the degradation of clopyralid on the anodic surface was studied
430 through a simple electrolysis and electrolysis but in the presence of tert-butanol. These
431 electrolyses, as well as an EF experiment in view of comparison, were made in the same
432 operating conditions, applying 50 mA of current during 120 min . Both electrolyses tests
433 achieved 10% of clopyralid removal, whereas EF led to 30% removal. These results
434 confirm again that the electrooxidation of clopyralid was negligible.

435

436 **3.7. Biodegradability of the electrolyzed soil washing effluents**

437 Due to the low mineralization yield, a longer EF treatment was considered in order to
438 improve the mineralization yield and the biodegradability of the wastewater after the

439 treatment. Two long electrolysis experiments were implemented at 50 and 200 mA and
 440 the generation of carboxylic acid was followed. In the literature, the ratio BOD_5/COD is
 441 usually employed to analyse the biodegradability of water samples (Zaghdoudi et al.,
 442 2017). If the ratio exceeds 0.4, the sample can be considered biodegradable (Carboneras
 443 et al., 2018). The obtained results are presented in Figs. 6 and 7 respectively. Experiments
 444 were carried out by adding 1 mM of ferrous ions and lasted 8 h.



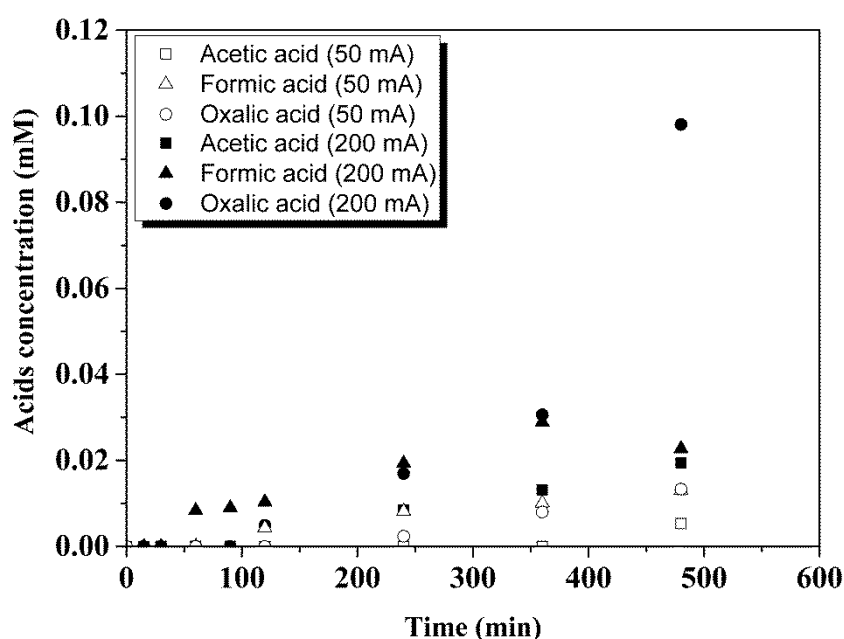
445

446 Figure 6. Time-courses of clopyralid degradation and its mineralization during EF at 50
 447 and 200 mA.

448

449 As can be seen in Fig. 6, when operating at a current of 200 mA, a higher mineralization
 450 efficiency and a higher degradation of clopyralid was obtained, reaching 30 and 80%
 451 respectively. These results could be related to the higher production of H_2O_2 when the
 452 system was operated at 200 mA. However, in spite of getting a good removal of
 453 clopyralid, the mineralization yield reached only around 30%. This result can be

454 explained by the formation of a too low concentration of $\bullet\text{OH}$ linked to a non-efficient
455 regeneration of ferrous ions to completely mineralize clopyralid (Aboudalle et al., 2018a).
456 The IC analysis showed the formation of 3 carboxylic acids: acetic, formic and oxalic
457 acids. When clopyralid was removed, these three carboxylic acids appeared, increasing
458 their concentration during the experiments, reaching the highest concentrations at the end
459 of the experiment. Fig. 7 shows the acids concentration along the experiments.



460
461 Figure 7. Evolution of carboxylic acid concentrations along EF reactions at 50 mA (empty
462 symbols) and at 200 mA (full symbols).

463
464 With regard to the cumulative acids production, the electrolysis carried out at 200 mA led
465 to the highest concentration, 0.10 mM for oxalic acid, a concentration about ten times
466 higher than those obtained after the electrolysis at 50 mA.
467 During the electrolysis at 200 mA, the rate of carboxylic acids, especially oxalic acid,
468 seemed to significantly increase from 360 min. It can be then expected that the
469 biodegradability of the effluent can be improved with the significant increase in the

470 production rate of such carboxylic acids. In order to ratify this hypothesis, the BOD₅/COD
471 ratios obtained after both experiments, carried out at 50 and 200 mA of current density,
472 were determined. Table SM-2 presents the initial and final BOD₅/COD ratios obtained in
473 the experiments carried out with 1 mM of ferrous ions and groundwater as a supporting
474 electrolyte at 50 and 200 mA.

475

476

477 The initial solution of clopyralid was not considered biodegradable because of its
478 BOD₅/COD ratio below 0.4. However, the initial value of this ratio, 0.33, means that
479 some biodegradable compounds were present in the commercial clopyralid formulation
480 (Fontmorin et al., 2014).

481 After 480 min of electrolysis at 200 mA the solution became biodegradable reaching
482 BOD₅/COD ratios of 0.48 and 0.39 when applying 200 and 50 mA respectively (Table
483 SM-2). This behaviour could be explained by the production of carboxylic acids
484 {Fernandez, 2008, Evaluation of carbon degradation during co-composting of exhausted
485 grape marc with different biowastes}. This improvement of the biodegradability can be
486 explained by the significant generation of carboxylic acids and especially oxalic acid that
487 can be easily metabolized by microorganisms (Fernández et al., 2008). Monitoring the
488 evolution of carboxylic acids during the electrolysis could be then an interesting
489 diagnostic tool for the estimation of biodegradability and could be easily inserted into the
490 process. Regarding the electrolysis at 50 mA, biodegradability of the electrolyzed
491 solution was nearly similar to the initial biodegradability, which can also be explained by
492 the low mineralization of the organic compounds and then the presence of by-products
493 structurally close to clopyralid (Mansour et al., 2012).

494

495 **4. CONCLUSIONS**

496 From this study, several conclusions can be extracted. Voltammetric study showed that
497 clopyralid was not electroactive and then was not degraded at the electrode surface by a
498 heterogeneous electron transfer. At a current of 200 mA, 80% of clopyralid was degraded
499 and mineralization yield reached 30 %, improving the biodegradability ratio BOD₅/COD
500 from 0.33 to 0.48 in 480 min. The evolution of the carboxylic acids was studied and the
501 results seemed to show that the improvement of biodegradability can be linked to a
502 significant increase of the carboxylic acids production rate and more especially oxalic
503 acid. The EF process can be carried out using groundwater as sustainable supporting
504 electrolyte. It allows the use of a natural resource, groundwater, avoiding the addition of
505 synthetic electrolytes and the increase of the salinity of the natural water bodies receiving
506 these effluents. The groundwater had a significant influence in the EF efficiency, reducing
507 the H₂O₂ production and, therefore, the efficiency of the EF process. The mineral salt that
508 presented the highest impact on the process was KI. In the studied operating conditions,
509 neither the initial catalyst concentration nor the oxygen flow rate had a significant
510 influence in the EF process. Because of that, an EF pre-treatment can be used to improve
511 the biodegradability of polluted soil washing effluent using groundwater as a supporting
512 electrolyte.

513

514 **5. Acknowledgements**

515 Authors wish to express their gratitude to the financial support from the Spanish Ministry
516 of Economy, Industry and Competitiveness and European Union through project
517 CTM2016-76197-R (AEI/FEDER, UE) and CYTEMA -Campus Científico y
518 Tecnológico de la Energía y el Medioambiente- for the pre-doc CYTEMA-Net mobility
519 grant of María Belén Carboneras.

521 6. References

- 522 Aboudalle, A., Djelal, H., Fourcade, F., Domergue, L., Assadi, A.A., Lendormi, T., Taha, S., Amrane,
523 A., 2018a. Metronidazole removal by means of a combined system coupling an electro-Fenton
524 process and a conventional biological treatment: By-products monitoring and performance
525 enhancement. *J. Hazard. Mater.* 359, 85-95.
- 526 Aboudalle, A., Fourcade, F., Assadi, A.A., Domergue, L., Djelal, H., Lendormi, T., Taha, S., Amrane,
527 A., 2018b. Reactive oxygen and iron species monitoring to investigate the electro-Fenton
528 performances. Impact of the electrochemical process on the biodegradability of metronidazole
529 and its by-products. *Chemosphere* 199, 486-494.
- 530 AFNOR, A.F.d.N., 1982. Essais des eaux: dosage du fer : méthode spectrométrique à la
531 phénanthroline - 1,10 : norme française homologuée NF T90-017., Paris, France.
- 532 Aydin, M.E., Aydin, S., Beduk, F., Ulvi, A., Bahadir, M., 2018. Accumulation of Micropollutants in
533 Aqueous Media and Sediment, A Risk Assessment for Konya Main Drainage Channel, Turkey.
534 *International Conference on Applied Human Factors and Ergonomics*. Springer, pp. 286-295.
- 535 Barrera-Díaz, C., Cañizares, P., Fernández, F., Natividad, R., Rodrigo, M., 2014. Electrochemical
536 advanced oxidation processes: an overview of the current applications to actual industrial
537 effluents. *J. Mex. Chem. Soc.* 58, 256-275.
- 538 Belen Carboneras, M., Villasenor, J., Jesus Fernandez-Morales, F., Andres Rodrigo, M., Canizares,
539 P., 2018. Biological treatment of wastewater polluted with an oxyfluorfen-based commercial
540 herbicide. *Chemosphere* 213, 244-251.
- 541 Beqqal, N., Yahya, M.S., Karbane, M., Guessous, A., El Kacemi, K., 2017. Kinetic study of the
542 degradation/mineralization of aqueous solutions contaminated with Rosuvastatin drug by
543 Electro-Fenton: Influence of experimental parameters. *J. Mat. Environ. Sci.* 8, 4399-4407.
- 544 Bortleson, G.C., Davis, D., 1997. Pesticides in selected small streams in the Puget Sound Basin,
545 1987-1995. US Geological Survey.
- 546 Bouaziz, I., Hamza, M., Sellami, A., Abdelhédi, R., Savall, A., Serrano, K.G., 2017. New hybrid process
547 combining adsorption on sawdust and electrooxidation using a BDD anode for the treatment of
548 dilute wastewater. *Sep. Purif. Technol.* 175, 1-8.
- 549 Brillas, E., Sirés, I., Oturan, M.A., 2009. Electro-Fenton process and related electrochemical
550 technologies based on Fenton's reaction chemistry. *Chem. Rev.* 109, 6570-6631.
- 551 Buxton, G.V., Greenstock, C.L., Helman, W.P., Ross, A.B., 1988. Critical review of rate constants for
552 reactions of hydrated electrons, hydrogen atoms and hydroxyl radicals ($\cdot\text{OH}/\cdot\text{O}^-$ in aqueous
553 solution. *J. Phys. Chem. Ref. Data* 17, 513-886.
- 554 Cano-Sancho, G., Ploteau, S., Matta, K., Adoamnei, E., Louis, G.B., Mendiola, J., Darai, E., Squifflet,
555 J., Le Bizec, B., Antignac, J.-P., 2019. Human epidemiological evidence about the associations
556 between exposure to organochlorine chemicals and endometriosis: Systematic review and
557 meta-analysis. *Environ. Int.* 123, 209-223.
- 558 Carboneras, M.B., Cañizares, P., Rodrigo, M.A., Villaseñor, J., Fernandez-Morales, F.J., 2018.
559 Improving biodegradability of soil washing effluents using anodic oxidation. *Bioresour. Technol.*
560 252, 1-6.
- 561 Chair, K., Bedoui, A., Bensalah, N., Fernández-Morales, F.J., Sáez, C., Cañizares, P., Rodrigo, M.A.,
562 2017a. Combining bioadsorption and photoelectrochemical oxidation for the treatment of soil-
563 washing effluents polluted with herbicide 2,4-D. *J. Chem. Technol. Biotechnol.* 92, 83-89.
- 564 Chair, K., Bedoui, A., Bensalah, N., Sáez, C., Fernández-Morales, F.J., Cotillas, S., Cañizares, P.,
565 Rodrigo, M.A., 2017b. Treatment of Soil-Washing Effluents Polluted with Herbicide Oxyfluorfen
566 by Combined Biosorption–Electrolysis. *Ind. Eng. Chem. Res.* 56, 1903-1910.
- 567 Chaplin, B.P., 2014. Critical review of electrochemical advanced oxidation processes for water
568 treatment applications. *Environ. Sci.: Processes Impacts* 16, 1182-1203.

569 Comninellis, C., Kapalka, A., Malato, S., Parsons, S.A., Poullos, I., Mantzavinos, D., 2008. Advanced
570 oxidation processes for water treatment: advances and trends for R&D J. Chem. Technol.
571 Biotechnol. 83, 769-776.

572 Dalle, A.A., Domergue, L., Fourcade, F., Assadi, A.A., Djelal, H., Lendormi, T., Soutrel, I., Taha, S.,
573 Amrane, A., 2017. Efficiency of DMSO as hydroxyl radical probe in an Electrochemical Advanced
574 Oxidation Process– Reactive oxygen species monitoring and impact of the current density.
575 Electrochim. Acta 246, 1-8.

576 Das, R.K., Golder, A.K., 2017. Impact of supporting electrolytes on the stability of TiO₂-Ti counter
577 electrode during H₂O₂ electrogeneration. Surf. Eng. Appl. Electrochem. 53, 570-579.

578 De Lucas, A., Rodriguez, L., Villasenor, J., Fernandez, F.J., 2007. Influence of industrial discharges
579 on the performance and population of a biological nutrient removal process. Biochem. Eng. J.
580 34, 51-61.

581 Diagne, M., Oturan, N., Oturan, M.A., 2007. Removal of methyl parathion from water by
582 electrochemically generated Fenton's reagent. Chemosphere 66, 841-848.

583 Do, J.-S., Yeh, W.-C., 1996. Paired electrooxidative degradation of phenol with in situ
584 electrogenerated hydrogen peroxide and hypochlorite. J. Appl. Electrochem. 26, 673-678.

585 Eisenberg, G., 1943. Colorimetric determination of hydrogen peroxide. Ind. Eng. Chem., Anal. Ed.
586 15, 327-328.

587 Feng, L., Oturan, N., Van Hullebusch, E.D., Esposito, G., Oturan, M.A., 2014. Degradation of anti-
588 inflammatory drug ketoprofen by electro-oxidation: comparison of electro-Fenton and anodic
589 oxidation processes. Environ. Sci. Pollut. Res. 21, 8406-8416.

590 Fernández, F.J., Sánchez-Arias, V., Villaseñor, J., Rodríguez, L., 2008. Evaluation of carbon
591 degradation during co-composting of exhausted grape marc with different biowastes.
592 Chemosphere 73, 670-677.

593 Fontmorin, J.-M., Siguié, J., Fourcade, F., Geneste, F., Floner, D., Soutrel, I., Amrane, A., 2014.
594 Combined electrochemical treatment/biological process for the removal of a commercial
595 herbicide solution, U46D®. Sep. Purif. Technol. 132, 704-711.

596 Ganzenko, O., Huguenot, D., Van Hullebusch, E.D., Esposito, G., Oturan, M.A., 2014.
597 Electrochemical advanced oxidation and biological processes for wastewater treatment: a
598 review of the combined approaches. Environ. Sci. Pollut. Res. 21, 8493-8524.

599 Garcia-Becerra, F.Y., Ortiz, I., 2018. Biodegradation of Emerging Organic Micropollutants in
600 Nonconventional Biological Wastewater Treatment: A Critical Review. Environ. Eng. Sci. 35,
601 1012-1036.

602 Gaur, N., Narasimhulu, K., PydiSetty, Y., 2018. Recent advances in the bio-remediation of persistent
603 organic pollutants and its effect on environment. J. Cleaner Prod. 198, 1602-1631.

604 Glaze, W.H., 1987. Drinking-water treatment with ozone. Environ. Sci. Technol. 21, 224-230.

605 Huang, C., Dong, C., Tang, Z., 1993. Advanced chemical oxidation: its present role and potential
606 future in hazardous waste treatment. Waste Manag. 13, 361-377.

607 Kumar, S., Kaushik, G., Dar, M.A., Nimesh, S., Lopez-Chuken, U.J., Villarreal-Chiu, J.F., 2018.
608 Microbial Degradation of Organophosphate Pesticides: A Review. Pedosphere 28, 190-208.

609 Liang, P., Rivallin, M., Cerneaux, S., Lacour, S., Petit, E., Cretin, M., 2016. Coupling cathodic Electro-
610 Fenton reaction to membrane filtration for AO7 dye degradation: A successful feasibility study.
611 J. Membr. Sci. 510, 182-190.

612 Liu, G., Li, L., Huang, X., Zheng, S., Xu, X., Liu, Z., Zhang, Y., Wang, J., Lin, H., Xu, D., 2018. Adsorption
613 and removal of organophosphorus pesticides from environmental water and soil samples by
614 using magnetic multi-walled carbon nanotubes@ organic framework ZIF-8. J. Mater. Sci., 1-12.

615 Loaiza-Ambuludi, S., Panizza, M., Oturan, N., Özcan, A., Oturan, M.A., 2013. Electro-Fenton
616 degradation of anti-inflammatory drug ibuprofen in hydroorganic medium. J. Electroanal. Chem.
617 702, 31-36.

618 Ma, J., Graham, N.J., 2000. Degradation of atrazine by manganese-catalysed ozonation—influence
619 of radical scavengers. Water Res. 34, 3822-3828.

620 Mansour, D., Fourcade, F., Bellakhal, N., Dachraoui, M., Hauchard, D., Amrane, A., 2012.
621 Biodegradability improvement of sulfamethazine solutions by means of an electro-Fenton
622 process. *Water, Air, Soil Pollut.* 223, 2023-2034.

623 Minerales, E., 1985. Calidad y contaminación de las aguas 475 subterráneas en España: informe de
624 síntesis. Instituto Geológico y Minero de España 476, 477.

625 Moreira, F.C., Boaventura, R.A., Brillas, E., Vilar, V.J., 2017. Electrochemical advanced oxidation
626 processes: a review on their application to synthetic and real wastewaters. *Appl. Catal., B* 202,
627 217-261.

628 Oller, I., Malato, S., Sánchez-Pérez, J., 2011. Combination of advanced oxidation processes and
629 biological treatments for wastewater decontamination—a review. *Sci. Total Environ.* 409, 4141-
630 4166.

631 Oturan, M.A., Pimentel, M., Oturan, N., Sirés, I., 2008. Reaction sequence for the mineralization of
632 the short-chain carboxylic acids usually formed upon cleavage of aromatics during
633 electrochemical Fenton treatment. *Electrochim. Acta* 54, 173-182.

634 Panizza, M., Cerisola, G., 2009. Electro-Fenton degradation of synthetic dyes. *Water Res.* 43, 339-
635 344.

636 Petrucci, E., Da Pozzo, A., Di Palma, L., 2016. On the ability to electrogenerate hydrogen peroxide
637 and to regenerate ferrous ions of three selected carbon-based cathodes for electro-Fenton
638 processes. *Chem. Eng. J.* 283, 750-758.

639 Pérez, J.F., Sáez, C., Llanos, J., Cañizares, P., López, C., Rodrigo, M.A., 2017. Improving the efficiency
640 of carbon cloth for the electrogeneration of H₂O₂: role of polytetrafluoroethylene and carbon
641 black loading. *Ind. Eng. Chem. Res.* 56, 12588-12595.

642 Pimentel, D., Levitan, L., 1986. Pesticides: amounts applied and amounts reaching pests. *Bioscience*
643 36, 86-91.

644 Pérez, G., Fernández-Alba, A., Urtiaga, A., Ortiz, I., 2010. Electro-oxidation of reverse osmosis
645 concentrates generated in tertiary water treatment. *Water Res.* 44, 2763-2772.

646 Sirés, I., Brillas, E., Oturan, M.A., Rodrigo, M.A., Panizza, M., 2014. Electrochemical advanced
647 oxidation processes: today and tomorrow. A review. *Environ. Sci. Pollut. Res.* 21, 8336-8367.

648 Tilman, D., Cassman, K.G., Matson, P.A., Naylor, R., Polasky, S., 2002. Agricultural sustainability and
649 intensive production practices. *Nature* 418, 671.

650 Urtiaga, A., Pérez, G., Ibáñez, R., Ortiz, I., 2013. Removal of pharmaceuticals from a WWTP
651 secondary effluent by ultrafiltration/reverse osmosis followed by electrochemical oxidation of
652 the RO concentrate. *Desalination* 331, 26-34.

653 Verma, J.P., Jaiswal, D.K., Sagar, R., 2014. Pesticide relevance and their microbial degradation: a-
654 state-of-art. *Rev. Environ. Sci. Bio/Technol.* 13, 429-466.

655 Verma, P., Verma, P., Sagar, R., 2013. Variations in N mineralization and herbaceous species
656 diversity due to sites, seasons, and N treatments in a seasonally dry tropical environment of
657 India. *For. Ecol. Manage.* 297, 15-26.

658 Wang, L., Yao, Y., Zhang, Z., Sun, L., Lu, W., Chen, W., Chen, H., 2014. Activated carbon fibers as an
659 excellent partner of Fenton catalyst for dyes decolorization by combination of adsorption and
660 oxidation. *Chem. Eng. J.* 251, 348-354.

661 Xie, H., Wang, X., Chen, J., Li, X., Jia, G., Zou, Y., Zhang, Y., Cui, Y., 2019. Occurrence, distribution
662 and ecological risks of antibiotics and pesticides in coastal waters around Liaodong Peninsula,
663 China. *Sci. Total Environ.* 656, 946-951.

664 Zaghdoudi, M., Fourcade, F., Soutrel, I., Floner, D., Amrane, A., Maghraoui-Meherzi, H., Geneste,
665 F., 2017. Direct and indirect electrochemical reduction prior to a biological treatment for
666 dimetridazole removal. *J. Hazard. Mater.* 335, 10-17.

667 Zhou, W., Gao, J., Ding, Y., Zhao, H., Meng, X., Wang, Y., Kou, K., Xu, Y., Wu, S., Qin, Y., 2018. Drastic
668 enhancement of H₂O₂ electro-generation by pulsed current for ibuprofen degradation: Strategy
669 based on decoupling study on H₂O₂ decomposition pathways. *Chem. Eng. J.* 338, 709-718.

670 Özcan, A., Oturan, M.A., Oturan, N., Şahin, Y., 2009. Removal of Acid Orange 7 from water by
671 electrochemically generated Fenton's reagent. *J. Hazard. Mater.* 163, 1213-1220.
672 Özcan, A., Şahin, Y., Koparal, A.S., Oturan, M.A., 2008. Carbon sponge as a new cathode material
673 for the electro-Fenton process: comparison with carbon felt cathode and application to
674 degradation of synthetic dye basic blue 3 in aqueous medium. *J. Electroanal. Chem.* 616, 71-78.

675

676